Colloids and Surfaces B: Biointerfaces 191 (2020) 111004

Contents lists available at ScienceDirect

Colloids and Surfaces B: Biointerfaces

journal homepage: www.elsevier.com/locate/colsurfb

A Novel Biochemical Study of Anti-Ageing Potential of *Eucalyptus Camaldulensis* Bark Waste Standardized Extract and Silver Nanoparticles

Rasha A. Radwan[a,*], Youssef A. El-Sherif[b], Maha M. Salama[c,d]

[a] Biochemistry Department, Faculty of Pharmacy, Sinai University-Kantara Branch, El Ismailia, 41611, Egypt
[b] Pharmaceutics and Pharmaceutical Technology Department, Faculty of Pharmacy, Heliopolis University, Cairo, 11361, Egypt
[c] Pharmacognosy Department, Faculty of Pharmacy, Cairo University, Cairo, 11562, Egypt
[d] Department of Pharmacognosy, Faculty of Pharmacy, The British University in Egypt (BUE), El-Shorouk City, 11837, Egypt

ARTICLE INFO

Keywords:
Anti-ageing
HPLC-standardized eucalyptus bark
Ag nanoparticles
Waste
Green synthesis

ABSTRACT

Eucalyptus camaldulensis Dehnh belongs to family Myrtaceae. They are massive in Egypt. Although reputed for high phenolic content, barks are considered waste. Ageing is a natural phenomenon caused by apoptosis and senescence resulting in wrinkles. The phytochemical analysis of the 70% ethanolic *Eucalyptus camaldulensis* bark extract (EBE) and evaluation of its anti-ageing potential and as silver nanoparticles (AgNPs) were conducted in this study. Ultra performance liquid chromatography / electrospray ionization mass spectrometry of EBE fingerprint revealed twenty compounds, where Rutin was major. EBE was standardized to contain 1.26 % Rutin. AgNPs synthesized by green synthesis, were characterized by transmission electron microscope and zeta potential measurement. Both EBE and AgNPs were subjected to MTT assay in HFB4 cells and cell cycle arrest. Flow cytometry was used to assess apoptosis and p16 ^{INK4a}. Genetic expression of p53 and p21 and telomerase level were determined. Anti-wrinkle enzyme assays were done. AgNps were spherical, 468.7 nm in size and with Poly dispersity index of 0.817 ± 0.129. EBE and AgNPs with IC_{50} 0.156 mg/mL ± 0.05 and 2.315 ± 0.07 µg/mL expressed significant difference in % of cells (DNA content) at G2/M, apoptotic cells numbers, p53 and p21expression and p16^{INK4a} vs aged cells ($P < 0.0001$). Both expressed significant increase in telomerase ($P < 0.0001$). They exhibited elastase, collagenase and tyrosinase inhibition (75 ± 4.3 and 75.9 ± 6.8 % at 300 µg/mL, 58 ± 4.8 and 63 ± 2.3, at 500 µg/mL, 51 ± 4.8 and 65 ± 5.87, at 500 µg/mL, respectively. Although it is considered waste, EBE and Ag NPs are anti-ageing candidates as they inhibit apoptosis, senescence and prevent wrinkles formation.

1. Introduction

Ageing is a natural phenomenon among human where there is failure in conservation of homeostasis and possibility of dying escalates [1,2]. Senescence is a cellular response that encounters the proliferation of aged or damaged cells has been considered a major cause of ageing-related diseases [3,4]. Mis-regulation of apoptosis is highly related to ageing and ageing-related diseases [5]. Ageing leads to disproportionality between collagen making and breakdown. Thereby, their productions decreases and at the same time the levels of collagen breaking enzymes increase. Ageing could be divided into 2 classes; intrinsic and extrinsic. Genetic factors cause the former while external ones are responsible for the latter. Examples of the latter are sun contact, smoking, diet, and routine. Photo-ageing is due to sun exposure resulting in profound crumples, coarse and dehydrated skin, black and light spots and deficiency of skin's pliability. Skin wrinkling is the major sign of ageing. Skin elasticity is considered the main factor in skin's health. Thereby, inadequate hormone balance and/or mutations, rigid skin, excessive stress and smoking might also lead to skin tension and wrinkling [6]. The exact mechanism of wrinkles development is unknown so far. However, continuous contact with extrinsic causes can result in enhancement of the expressions of enzymes which in turn cause collagen destruction and deficiencies in dermis structure and hence wrinkle formation. It is worth mentioning that ageing process usually involves the activity of enzymes like elastase, collagenase and tyrosinase enzymes [7]. The concept of anti-ageing has been modified from only escalating life cycle to health expectancy prolongation, in the sense that there is more focus on the value of life. This approach is in accordance with natural ageing and prevention of pathological ageing, which is associated with disorders. The use of conventional drugs for skin ageing has led to several adverse effects in addition to the high cost. Natural products are a source of lead compounds that are safe and

* Corresponding author at: Biochemistry Department, Faculty of Pharmacy, Sinai University-Kantara Branch, El Ismailia, 41611, Egypt.
E-mail addresses: rashaaradwan@hotmail.com (R.A. Radwan), youssef.elsherif@hu.edu.eg (Y.A. El-Sherif), maha.salama@pharma.cu.edu.eg (M.M. Salama).

https://doi.org/10.1016/j.colsurfb.2020.111004
Received 17 December 2019; Received in revised form 25 March 2020; Accepted 26 March 2020
Available online 14 April 2020
0927-7765/

affordable with reported antioxidant activity; in particular its polyphenolic compounds. Furthermore, many of the herbal medicines are reported for their anti-ageing potential. Moreover, it has been reported several times that some medicinal herbs are efficient in treatment or prevention of neurological disorders associated with ageing [8–10].

Eucalyptus camaldulensis Dehnh (the River Red Gum) family Myrtaceae, is a well-known tree growing at the Delta region in Egypt. They exist on almost every roadside. In spite of being discarded and considered as waste, it has been proved through High Pressure liquid chromatography / electrospray ionization mass spectrometry (HPLC-ESI-MS) technique that the bark of *E. globulus* are rich in polyphenolic compounds [11]. In addition,another study was conducted [12] on the polyphenolic constituents of the bark from the ether soluble fraction of methanolic extracts of *E camaldulensis, E. globulus* and *E. rudis* evidenced the presence of different phenolic classes with different ratios in the three studied species. Furthermore, the antioxidant activity of different parts of the tree has been reported. In addition, the ethyl acetate fraction of the leaves of *E. camadulensis* expressed a potent antimicrobial and anti schistosomal activity. The activity was attributed to phenolic compounds of different classes: flavonoids, Gallic acid (GA) and Galloyl derivatives identified through structure elucidation [13,14]. Moreover, the aqueous acetone extract of the leaves of *E.camadulensis* recorded cytotoxic and antioxidant activity in a dose-dependent manner [15]. Moreover, the phloroglucinol isolated from the leaves of *E. sinerea*. exhibited anti- proliferative activity [16]. Additionally, the *n*-hexane fraction of the stem bark of *E. camadulensis* demonstrated potent anti-inflammatory effect [17].

Recently, vast attention has been paid to nanomedicines, as they have a large scale of applications [18]. Incorporation of natural products into nanoparticles is a favorable approach. It is simple, efficient, inexpensive and sustainable [19,20]. Silver nanoparticles (AgNPs) constitute an important integral part of nanomedicine. Green synthesis of nanoparticles utilizes the use of microorganisms and plants, and benefit from the ability of these organisms as reducing agents [21]. Thereby, phyto constituents and microorganisms incorporated are capable of reducing silver ions to nascent silver and shield the formed nanoparticles [22]. They act also as capping agent which in turn encounters several advantages; as preventing the agglomeration of the nanoparticles, decreasing toxicity, and improving antimicrobial action and give a synergistic antimicrobial effect if the formed particles have already an antimicrobial activity. In addition, AgNPs do not make alterations on living cells. Thereby, they are incapable of causing microbial resistance. Besides, they are able to attach to cell walls and modify cellular respiration [22]. Furthermore, they enhance *in-vitro* activities [23,24]. Silver nanoparticles were evaluated for its anti-ageing effect in previous studies [21,25,26] and in cosmetic preparations in other studies [25,27]

This work covers 3 dimensions: First, it undergoes in depth identification of *Eucalyptus camadulensis* bark extract (EBE) in 70% ethanol *via* Ultra performance liquid chromatography / electrospray ionization mass spectrometry (UPLC-ESI-MS/MS), along with its standardization by applying HPLC technique. Second, formulation of extract into AgNPs through green synthesis. Third, it assesses the anti-ageing potential of both extract as well AgNPs. Therefore, this study sheds a light on the reuse of waste (bark) as promising pharmaceutical product.

2. Materials & Methods

2.1. Materials and extraction

All reagents in the current investigation were purchased from (Sigma-Aldrich, Germany). The *Eucalyptus camadulensis* Dehnh grows in the botanical garden, Heliopolis University. The plant was authenticated by Dr. Saber Hendawy in the botanical garden, Heliopolis University, Cairo-Belbeis Desert Road from Cairo-Ismailia Desert, El Salam City. The identity of the plant was further authenticated by Therese Labib, consultant of Plant Taxonomy, Ministry of Agriculture, El- Orman Botanical Garden, Giza, Egypt. (Voucher specimen number 4.2.2017). The bark was collected from December 2017 till March 2018. Two Kg of the bark were powdered and macerated in 70% ethanol (4Lx3). The combined extract was evaporated under vacuum at 60°C and kept in the desiccator for further study.

2.2. Estimation of total phenolic and flavonoid contents

2.2.1. Standards and samples preparation

GA is the standard for total phenolics. Rutin is the standard for total flavonoids. GA stock solution of 1 mg/mL in methanol was prepared, and 7 serial dilutions were prepared in the concentrations of 500, 250, 125, 62.5, 31.2, 15.6, and 7.8 µg/mL. Rutin stock solution of 1 mg/mL in methanol was prepared, and 6 serial dilutions were prepared in the concentrations of 1000, 500, 250, 150, 100, and 50 µg/mL. Samples were prepared in concentration of 1 mg/mL methanol and measured using micro plate reader FluoStar Omega (BMG Lab tech, Germany) at 630 nm (GA) & 510 nm (Rutin) [28,29].

2.3. Qualitative determination and standardization of the extract by HPLC-PDA

Waters 2690 Alliance HPLC system equipped with a Waters 996, PDA detector was used. Column C_{18} luna: 4.6 x 250 mm, 3 µm, mobile phase: 1% Acetic acid: acetonitrile (Gradient elution), flow rate: 1 mL/min, temperature: 25°C and λ_{max} 270-400 nm were used. Luteolin, GA, Catechin, *Epi* catechin, Rutin, Quercetin and Ellagic acid were used as standards. Each concentration was filtered on 0.22 syringe filter then 10 µl was injected.

2.3.1. Sample preparation

100 mg/mL stock solution was prepared. 1 mLin 10 mLvolumetric flask completed with methanol. Final concentration was 10 mg/mL. 10 µl sample was injected

2.3.2. Construction of the standard calibration curve

A stock solution was prepared by dissolving Rutin in methanol (1.3 mg/mL). Serial dilutions from Rutin: 25, 50, 75, 100, 125ug/mL were further prepared. 10ul was injected. A standard calibration curve was established. Each sample was injected in triplicates at λ_{max} 353 nm. Extract concentration was 10 mg/mL.

2.4. UPLC-ESI-MS/MS conditions

The chromatographic separation was achieved using Waters ACQUITY QSM UPLC system equipped with reverse phase C-18 column (ACQUITY UPLC - BEH C18, 1.7 µm particle size - 2.1 × 50 mm Column. The mobile phase (A) was Water + 0.1 % Formic acid and the mobile phase (B) was Methanol + 0.1% Formic acid. Elution was performed at 0.95 mL min^{-1} gradient solvent B: 0–2 min, 10%, 2–5 min, 30%; 5–15 min, 70 %; 15-25 min, 90%; 25–29 min, 100 % and 29–32, min. 10%. The flow rate of the mobile phase was 0.2 mL/min. The injection volume was 10 µL. Column temperature was 30°C and column pressure was 22.9 bar. The analysis was carried out using a triple quadruple mass spectrometer (Xevo TQ-D, Waters Corp., Milford, MA, USA) with an ESI source. The mass spectrometer was operated in both negative & positive ion modes with the following conditions: source temperature 150 °C, cone voltage 30 eV, capillary voltage 3 kV, disolvation temperature 440 °C, cone gas flow 50 L/h, and disolvation gas flow 900 L/h. Mass spectra were detected in the ESI between 100–1000 *m/z*. The peaks and spectra were processed using the Maslynx 4.1 software and tentatively identified by comparing their retention times (TR), mass spectra, and MS/MS fragmentation of the peaks in the samples with those of the reported data.

2.5. Preparation of AgNPs and measuring nanoparticles parameters

Nanoparticles were prepared by silver reduction method which is considered a green synthesis method as follows: 1 g of EBE was dissolved in 10 mL ethanol by stirring on a magnetic stirrer (WiseMSH-20A, Germany) at 500 rpm at 25 °C. The solution was filtered to remove any un-dissolved bark extract parts. EBE solution was dropped over 10 mL of 0.01 M silver nitrate while stirring on a magnetic stirrer at 1000 rpm. Stirring continued for overnight at 25 °C [30]. The nanoparticles size and shape were studied using transmission electron microscope (TEM) (1230, JEOL, Tokyo, Japan). They were assessed for their particle size and Poly dispersity Index (PDI) by Malvern Zeta Sizer (ZS-90, Malvern Instrument, UK) in the central lab at Faculty of Pharmacy, Cairo University. AgNPs were further subjected to HPLC analysis to test the presence of EBE.

2.6. Markers of ageing

2.6.1. In-vitro testing on cell lines

2.6.1.1. Ageing Model and MTT assay. Ageing model incorporated the monolayer normal human fibroblast cell lines (HFB4) (Vaccera Giza, Egypt). They were cultivated in 75 cm^2 and incubated at 37 °C in 5% humidified CO_2. They were trypsinized with 0.25% trypsin and 0.025% EDTA and re-suspended (subculture) with Dulbecco's modified eagle medium (DMEM) with 10% fetal bovine serum (FBS). Then, they were split into 3 flasks. Flasks were incubated at 37 °C in humidified CO_2 until complete confluent cells were formed. After that three flasks were divided into seven flasks [31]. Samples tested were as follows; S1: H_2O_2 then AgNPs were added (testing treatment potential), S2: H_2O_2 then EBE were added (testing treatment potential), S3: Ag NPs then H_2O_2 were added (testing prophylactic potential), S4: EBE then H_2O_2 were added (testing prophylactic potential), S5: Ascorbic Acid (positive control) then H_2O_2 were added, S6: H_2O_2 was only added and S7: untreated cells. The cytotoxic effect of EBE and AgNPs were tested with MTT assay Kit ab211091 (Abcam, USA) in triplicates. The IC_{50} (concentration necessary for 50% inhibition of the enzyme activity) values were expressed as the mean ± SD. These values were further incorporated as their respective doses in the rest of EBE and AgNPs *in-vitro* testing.

2.6.1.2. Cell Cycle arrest analysis. All 7 samples were subjected to cell cycle analysis by quantification of DNA using ab139418Propidium iodide flow cytometry kit (Abcam, USA) using BD FACSCalibur Flow Cytometer (BD Biosciences, San Diego, CA, USA).

2.6.1.3. Apoptosis detection. All 7 samples were subjected to apoptosis determination using Annexin V-FITC Apoptosis Detection Kit (Biovision, USA) using BD FACSCalibur Flow Cytometer (BD Biosciences, San Diego, CA, USA).

2.6.1.4. Genetic expression of p53 and p21. First m RNA of p53 and p21 are isolated using RNeasy extraction kit (Qiagen, Germany).About 1×10^6 cells, are disrupted in Buffer RLT containing guanidine thiocyanate and homogenized. Ethanol is then added to the lysate, to help selective binding of RNA to the RNeasy membrane. Total RNA is then bound to the RNeasy Mini spin columns and washing is done several times. Consequently, high quality RNA is eluted in RNase-free water. Genetic expressions of p53 and p21 are carried out using The MIscript One-Step Real Time Polymerase Chain Reaction (RT-PCR) Kit with SYBR® Green (BioRad, USA) as follows; 25 µl 2X SYBR® Green RT-PCR Reaction Mix was mixed with (10 µM) of Forward primer and (10 µM) of Reverse primer.10 µl of 100 ng RNA template followed by 1 µl of MIscript Reverse Transcriptase for One-Step RT-PCR and 11 µl Nuclease-free H2O. Complete reaction mix is incubated in a real-time thermal detection system Rotor-gene Q RT- PCR system (Qiagen, Switzerland) as follows; cDNA synthesis: 10 min at 50 °C, MIscript Reverse transcriptase inactivation: 5 min at 95 °C,PCR cycling and detection (30 to 45 cycles): 10 sec at 95 °C and30 sec at 55 °C to 60 °C. The method for data interpretation used was measuring the difference in cycle threshold (ΔCt) value using Glyceraldehyde-3-phosphate dehydrogenase (GAPDH) as control. The Rotor-gene Q RT- PCR system with Q-Rex Software version 1.1

2.6.1.5. Percentage of p16 ^{INK4a} determination. The $p16^{INK4a}$ concentrations in all 7 samples were determined using Anti p16 antibodies, human (Miltenyi Biotech, Germany) using BD FACSCalibur Flow Cytometer (BD Biosciences, San Diego, CA, USA).

2.6.1.6. Telomerase determination. Telomerase was measured in all 7 samples quantitatively using Telomerase reverse transcriptase (TERT) ELISA kit (Biovision, USA) using an ELX 808 instrument (Bio-Tek Instrumental, Italy).

2.6.2. Estimation of elastase and collagenase inhibition

The anti-elastase and anti-collagenase activities of EBE and AgNPs were estimated according to [26] using an ELX 808 instrument (Bio-Tek Instrumental, Italy). The principal of the anti-elastase assay involves the inhibition of the elastase conversion of N-Succinyl-Ala-Ala-Ala-p-nitroanilide to p-Nitroanilide. The principal of the anti-collagenase assay involves the inhibition of the collagenase hydrolysis of 2-furanacryloyl-l-leucylglycyl-l-prolyl-l-alanine (FALGPA) to FAL and Gly-Ala -Pro. The percentage inhibition for both enzymes was calculated as follows: [(A control(without inhibitor)- A sample(with inhibitor))/A control] x 100 [32,33].

2.6.3. Estimation of tyrosinase inhibition

The anti-tyrosinase activities of the EBE and AgNPs were measured according to [26] using an ELX 808 instrument (Bio-Tek Instrumental, Italy). The principal of the anti-tyrosinase assay involves the inhibition of the tyrosinase conversion ofL3, 4-dihydroxyphenylalanine (L-DOPA) to dopachrome. The percentage inhibition was calculated as for elastase and collagenase [34].

2.7. Statistical analysis

Data were evaluated using analysis of variance (ANOVA). All experiments were performed three times. Differences are considered significant at $P < 0.05$. The IC_{50} values were estimated from linear regression curve. The difference in the effects of EBE and AgNPs on ageing enzyme inhibition were evaluated using ANOVA followed by Tukey's honest significant difference post hoc test at $p < 0.05$ [35]. Pearson correlation coefficients at $P < 0.05$ test was used to assess association between the total phenolic and flavonoid contents and the inhibitory effect of enzymes. SPSS v. 22.0 (IBM, Chicago, USA) was used for analysis.

3. Results

3.1. Estimation of total phenolic and flavonoid contents

Total phenolic & flavonoid contents were 434.8 mg/g GA equivalent ± 35.4 & 346.3 mg / g Rutin equivalent ± 0.03, respectively.

3.2. UPLC-ESI-MS/MS analysis

The examination of EBE profile with LC/MS/MS in negative and positive ion modes results are presented in Table 1.

3.3. Nanoparticle parameters measurement

TEM of AgNPs showed particles in the nano range with a spherical shape as shown in Fig. 1. Malvern Zeta Sizer showed that the

Table 1
Peak assignments of metabolites in *EBE* using UPLC-MS/MS in negative & positive modes.

Peak %	TR (min)	[M-H]-	MS^2	Tentative identification
1-Hydrolysable tannins Ellagic acid & ellagic acid derivatives				
1%	19.8	463.8	301.6, 257.7, 185.1	Ellagic acid hexoside
1%	31.5	301	284, 255.2, 184.7	Ellagic acid
Ellagitannins				
1%	14.2	633.2	317. 6, 301.3, 251.4, 167.4	Galloyl HHDP –hexoside (corilagin)
1%	22.6	953.6	623. 6, 298.5, 168.	valoneoyl-digalloyl-hexoside
2%	1.23	934.	631.1, 471.8, 301.7	castalagin
		339.2	322, 182, 109	HHDP
2-Condensed tannins				
1%	8.2	289.3	245.4, 221. 6, 179.8	(*epi*) catechin
3-Phloroglucinol				
11%	12.39	498.	313.4, 183, 169.2	Eucaglobulin
1%	18.3	471.1	453.7 (-CH3), 427.2 (-CHOO), 357.3, 219.5	Formylated phloroglucinol derivatives
6%	9.8	537.2	345.2 (-162-OCH2), 231, 167.2	Phloroglucinol glucoside derivative (cypellocarpin B)
4-Hydroxybenzioic & cinnamic acid derivatives				
4%	9.6	169	125, 79.3	Gallic acid
1%	12.2	195.5	178.8, 148.9	Ferulic acid
2%	10.66	353.2	191.1 (Quinic acid), 177, 135.4	caffeoylquinic acid
5-Flavonoids				
1%	8.6	589.6	447.1(-rhamnosyl),170 (gallic)	Quercetin- galloyl-rhamnoside
12%	12.9	610.6	464 (-rhamnosyl), 301, 283.4	Quercetin-rutinoside (rutin)
1%	11.7	433	300.8, 235, 152.2	Quercetin pentoside
1%	8	446.9	413, 300.1	Quercetin rhamnoside (astragalin)
1%	5.5	460.60	399, 315.3	(*iso*)Rhamnetin rhamnoside
6%	25.1	301	257.4, 229. 2, 185.1	quercetin
5%	23	287.1	269, 250.7	Luteolin
7%	26.7	317.1	302.1, 274.1, 228.1, 137	(*iso*) rhamnetin
6-Unidentified compounds				
1%	9	513.5	315, 296.4, 166.1, 117.8	unidentified
1%	27	621.3	522	unidentified

nanoparticle size was 468.7 nm with PDI of 0.817 ± 0.129. When EBE was unloaded from AgNPs, using Rutin was found to be the major component recovered accounting to 28 μg/ml indicating that the extract is loaded on the Ag particle.

3.4. Markers of anti-ageing

3.4.1. In vitro Cell testing

3.4.1.1. MTT assay. MTT results of EBE and its Ag NPs showed IC_{50} of 0.156 mg/mL ± 0.05 and 2.315 ± 0.07 mg/ml, respectively.

3.4.1.2. Cell cycle arrest analysis. It was observed that cell growth was arrested at G2/M phase. In this phase, there was a prominent significant difference in % of cells between cells treated with EBE and AgNPs S1,S2 and cells treated with Ascorbic acid (anti-ageing control drug) S5 $P < 0.0001$. Moreover, there was a prominent significant difference in % of cells between S1,S2 and aged cells (S6) $P < 0.0001$. Interestingly, no significant difference existed between S1 and S7 or between S2 and S7 as shown in Fig. 2. Furthermore, there was a significant increase % of cells between S3 and S5,S6 and S7 $P < 0.0001$, respectively.Moreover, there was a significant increase in % of cells between S4 and S5,S6 and S7 $P < 0.0001$, respectively.

3.4.1.3. Apoptosis Detection. Percentage of apoptotic cells at different stages of apoptosis are presented in Fig. 3. A prominent significant decrease in % of apoptotic cells ($P < 0.0001$) between S1 and S6 at all stages of apoptosis was clear in the current study. Moreover, this same significant decrease existed between S2 and S6. Interestingly, significant increase in potency existed between S1 and S2 on one side and S5 (the anti-ageing drug) on the other side ($P < 0.0001$).

3.4.1.4. Genetic expression of p53 and p21. Folds change of genetic expression of p53 and p21 are represented in Fig. 4. It was observed that there is a significant decrease in the expression of p53 in samples S1, S2, S3, S4 vs S6 at $P < 0.0001$. Moreover, there was a significant increase in potency between S1, S2, S3, S4 and vs S5 in decreasing expression of p53 at $P < 0.0001$. Furthermore, there was a significant difference in expression of p53 between S1 and S2, S1 and S3 and S1

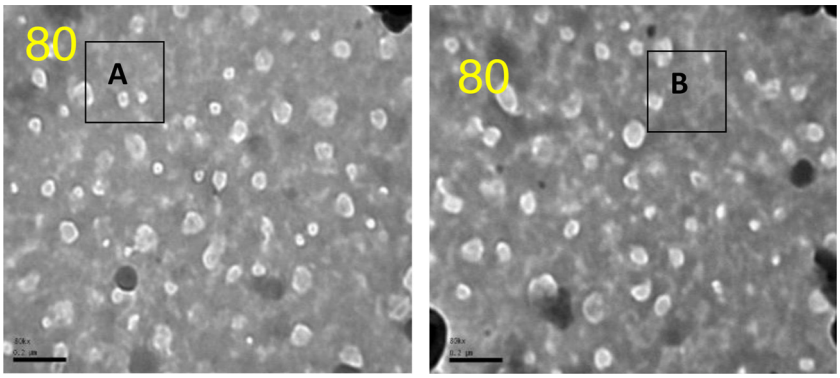

Fig. 1. TEM micrograph of AgNPs with magnification power 80 Kx in A and B.

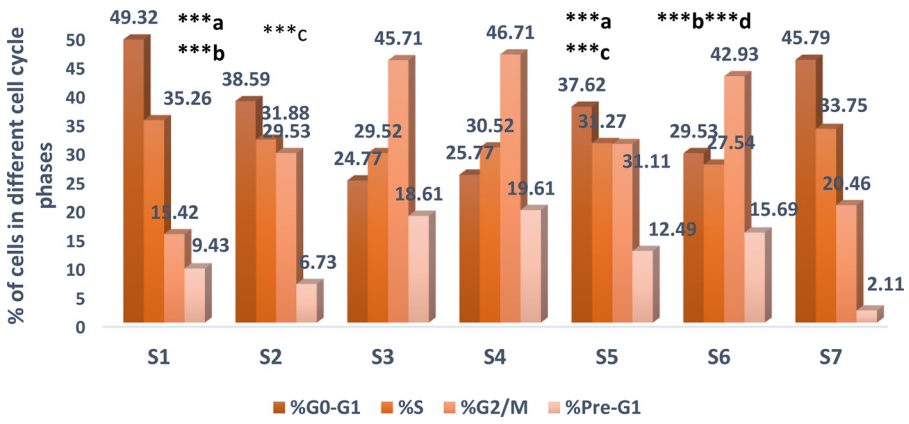

Fig. 2. Percentage (%)of cells in different phases of cell cycle when applying EBE and Ag NPs. ***a: Significant difference in % of cells between S1 and S5 $P < 0.0001$. ***b: Significant difference in in % of cells between S1 and S6 $P < 0.0001$. ***c: Significant difference in % of cells between S2 and S5 $P < 0.0001$. ***d: Significant difference in % of cells between S2 and S6 $P < 0.0001$.

and S4 at $P < 0.001$. Moreover, S2 exhibited significant difference with S3 and S4 at $P < 0.0001$, respectively.On the other hand, there was no significant difference between S3 and S4. It was clear that there is a significant decrease in the expression of p21 in samples S1, S2 vs S6 at $P < 0.0001$. Likewise, there was a significant difference in expression of p21 between S1 and S2 at $P < 0.05$, S1 and S3 and S1 and S4 at $P < 0.0001$, respectively. Moreover, S2 exhibited significant difference with S3 and S4 at $P < 0.0001$, respectively. On the other hand, there was no significant difference between S3 and S4.Hence, treatment potential with S1 and S2 was more potent than prophylactic potential with S3 and S4 in decreasing expression of p53 and p21. Moreover, there was a significant increase in potency between S1 and S2 vs S5 in decreasing expression of p21 at $P < 0.0001$, hence inhibiting apoptosis and ageing.

3.4.1.5. Percentage of p16 ^{INK4a} determination. Levels of $p16^{INK4a}$ are presented in Table 2. Levels of $p16^{INK4a}$ in S1 and S2 were significantly decreased compared to S6 $P < 0.0001$. Furthermore, this significant decrease was explored in S1 and S2 compared to S5 $P < 0.001$. Interestingly, there is no significant difference between S1 and S2 compared to S7 regarding $p16^{INK4a}$ concentration. Moreover, there was a significant difference in levels of $p16^{INK4a}$ between S1 and S2 $P < 0.001$, S1 and S3 and S1 and S4 at $P < 0.0001$, respectively. Moreover, S2 exhibited significant difference with S3 and S4 at $P < 0.0001$, respectively. On the other hand, there was no significant difference between S3 and S4.Hence, treatment potential with S1 and S2 was more potent than prophylactic potential with S3 and S4 in decreasing level of $p16^{INK4a}$.

3.4.1.6. Telomerase determination. Telomerase concentrations are presented in Table 2. The significant increase in telomerase concentration was clear between S1, S2, S3, S4 and S7 compared to S6 $P < 0.0001$, respectively. Moreover, there was a significant increase in telomerase concentration in S1, S2, S3, S4 compared to S5 $P < 0.0001$, respectively. Additionally, there was a significant difference in telomerase concentration between S1 and S2 $P < 0.001$, S1 and S3 and S1 and S4 at $P < 0.0001$, respectively. Moreover, S2 exhibited significant difference with S3 and S4 at $P < 0.0001$, respectively. Conversely, there was no significant difference between S3 and S4. In conclusion, treatment potential with S1 and S2 was more potent than prophylactic potential with S3 and S4 in increasing telomerase concentration.

3.4.2. Estimation of elastase and collagenase inhibitions

Rutin, AgNPs and EBE inhibited elastase (88. 8 ± 7.5, 75.9 ± 6.8 and 75 ± 4.3 %, respectively) at 300 μg /mL Fig. 5. Their IC_{50} values were 110.95 ± 8.9, 132.82 ± 8.3 and 343.3 ± 5.4 μg/mL, respectively. Moreover, there was a significant positive correlation in elastase inhibition between EBE and flavonoid and phenolic contents ($r = 0.988$, $P = 0.01$ and $r = 0.99$, $P = 0.001$, respectively). Same correlation existed in elastase inhibition with AgNPs($r = 0.921$, $P = 0.01$ and $r = 0.91$, $P = 0.001$, respectively). Furthermore, Rutin, AgNPs and the EBE exhibited anti-collagenase activity (63.8 ± 3.1, 63 ± 2.3 and 58 ± 4.8, respectively at 500 μg/mL Fig. 5. Their IC_{50} values were 307.27 ± 5.8, 279.34 ± 5.4 and 416.3 ± 5.6 μg/mL, respectively. In addition, there was a strong significant positive correlations between the total flavonoid and phenolic contents and the % of collagenase inhibition exerted by EBE ($r = 0.991$, $P = 0.008$ and $r = 0.996$, $P = 0.003$, respectively) and AgNPs ($r = 0.964$, $P = 0.006$ and $r = 0.925$, $P = 0.005$, respectively). Interestingly, no significant difference existed in the % inhibition of elastase and collagenase between Rutin, AgNPs and EBE.

3.4.3. Estimation of tyrosinase inhibition

The tyrosinase inhibitory effects of Rutin, AgNPs and the EBE were

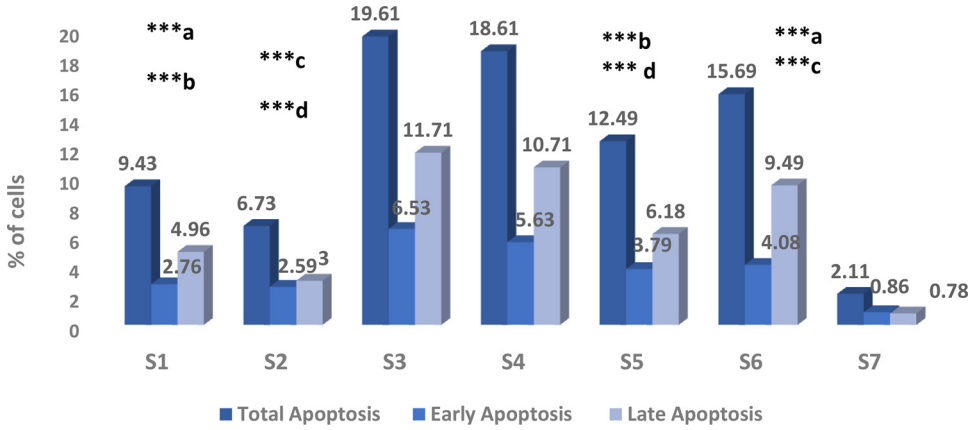

Fig. 3. Percentage of cells in different apoptotic phases when applying EBE and AgNPs ***a: Significant decrease in % of apoptotic cells ($P < 0.0001$) between S1 and S6. ***b: Significant difference in % of apoptotic cells ($P < 0.0001$) between S1 and S5. ***c: Significant decrease in % of apoptotic cells ($P < 0.0001$) between S2 and S6. ***d: Significant difference in % of apoptotic cells ($P < 0.0001$) between S2 and S5.

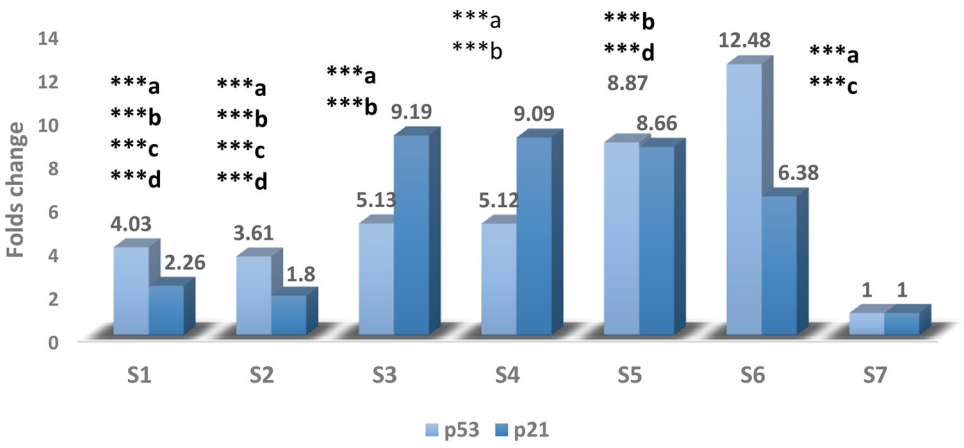

Fig. 4. Folds change of genetic expression of p53 and p21 when applying EBE and Ag NPs. ***a: Significant decrease in the expression of p53 in samples S1, S2, S3, S4 vs S6 at $P < 0.0001$. ***b: Significant increase in potency between S1, S2, S3, S4 and vs S5 in decreasing expression of p53at $P < 0.0001$.. ***c: Significant decrease in the expression of p21 in samples S1and S2 vs S6 at $P < 0.0001$. ***d: Significant increase in potency between S1 and S2 vs S5 in decreasing expression of p21at $P < 0.0001$.

Table 2
$p16^{INK4a}$ % determination and telomerase concentration on treatment of Hfb4 cells with EBE and AgNPs.

	p16_INK4a %	Telomerase ng/mL
S1	8.9	1.74 ± 0.021
S2	8.1	1.9 ± 0.025
S3	12.1	1.44 ± 0.043
S4	12.2	1.45 ± 0.033
S5	10.4	1.25 ± 0.022
S6	12. 7	1.28 ± 0.020
S7	8.7	2.17 ± 0.04

found to be (65.16 ± 5.77, 65 ± 5.87 and 51 ± 4.8, respectively) at 500 µg/mL Fig. 5. Rutin, AgNPs and EBE showed no significant difference between their % inhibition values. Their IC_{50} values were 215.1 ± 6.9, 315.9 ± 8.6 and 555.55 ± 5.87 µg /mLml. Furthermore, strong significant positive correlations between the total flavonoid and phenolic contents and the tyrosinase inhibition exerted by EBE and AgNPs were observed; ($r = 0.992$, $P = 0.030$ and $r = 0.982$, $P = 0.020$,) ($r = 0.962$, $P = 0.035$ and $r = 0.981$, $P = 0.030$), respectively.

4. Discussion

Nowadays, the use of natural products has become an inevitable necessity. The compounds in EBE were identified in both negative & positive modes. However, the negative mode displayed more peaks. Table 1 displayed the detection of 22 compounds, of which 20 were identified. Selection of peaks was based on the major peaks as well as the literature review. The phenolic compounds were classified by matching their mass fragmentation with that of the reported phenolics from the literature. The main detected classes were, Ellagic acid derivatives, Ellagitannins, Phloroglucinol derivatives, Hydroxybenzoic acid & Hydroxycinnamic acid derivatives as well as flavonoids of mainly flavonol nucleus.

4.1. Hydrolysable tannins

4.1.1. Ellagic acid & Ellagic acid conjugates

These were represented by two peaks based on their mass fragmentation pattern. The first peak (TR = 31.49 min.), had [M - H]- at *m/z* 301 with the characteristic (mass spectroscopy) MS^2 fragmentation at *m/z* 257, 229, and 185, identical to Ellagic acid fragments [36]. Similarly, another signal at (TR = 19.72 min.), m/z 463.7919 [M-H]- the mass product showed a characteristic deprotonated peak at 301 amu, reflecting the removal of an hexoside residue, the equivalent deprotonated ion yields at *m/z* 257and 185 amu which are characteristic for Ellagic acid conjugates [37]. Therefore, this compound is tentatively identified as ellagic acid hexoside.

4.1.2. Ellagitannins

This group of hydrolysable tannins is distinguished by one or more hexahydroxydiphenoyl (HHDP) on a polyol moiety center mainly glucose [38]. The HHDP group are easily hydrolyzed, releasing a stable ellagic acid which is a dilactone form of hexahydroxydiphenic acid.

They were represented by three peaks; the first peak with [M-H]-, m/z 633 was detected at (TR = 14.15 min.). The MS^2 revealed peaks at m/z 317amu due to the loss of hexose (-162) with consequent loss of galloyol moiety (-152). There is another characteristic peak at 167 amu that corresponds to [GA-2 H]. Moreover, the characteristic ion at *m/z* 301 coincides with the fragmentation pathway of ellagitannins.

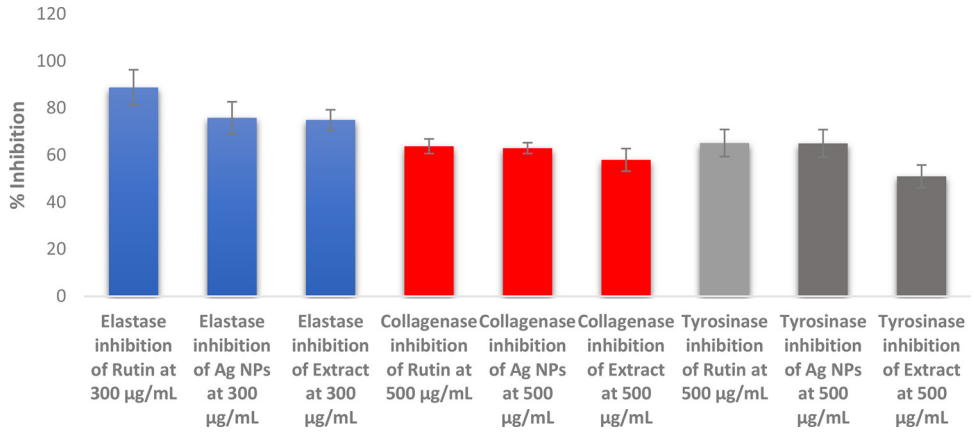

Fig. 5. EBE and AgNPs inhibition of the different enzymes.

Therefore, this compound is tentatively identified as galloyl HHDP-hexose (corilagin) [39]. Likewise, peak at (TR = 1.23 min.), $[M+H]^+$ 934, giving daughter ions at 631amu [M-302] equivalent to the loss of Ellagic acid, another peak at m/z 301amu that corresponds to [M-galloyl HHDP-hexose]. Therefore, this compound is presumably identified as castalagin. The third peak emerged at (TR = 11.15 min.) in the negative mode, showed a molecular ion at m/z 953.62 that produced MS^2 fragmentation pattern distinguished at 623 amu, corresponding to [M-162- 169] due to the consequent loss of hexose followed by GA, respectively. Another peak was detected at 298 amu that is equivalent to [Ellagic acid -2 H]. Finally, There is another peak at 168.9 [GA –H]. In this way, we can tentatively identify the structure as valoneoyl- digalloyl- hexoside [40]

4.2. Condensed tannins

This was represented by only one peak; with (TR = 8.18 min.) ([M–H] $^-$ at m/z 289. 27) exhibited characteristic MS^2 fragments at m/z 247.42 (loss of COO), m/z 179.78 amu and was tentatively identified as (*Epi*) catechin.

4.2.1. Phloroglucinols

These were represented by three peaks: the first one was detected at (TR = 22.57 min.), with molecular ion peak [M-H] – 497. The fragmentation pattern of this compound showed an ion at; m/z 313.35 amu that corresponded to the loss of (M-galloyoyl hexoside) another deprotonated ion at m/z 182.9 amu equivalent (oleuropeic acid moiety). Finally, it gave rise to 169.1496 (GA). This mass fragmentation spectrum coincides with those of eucaglobulin. Hence, this compound is tentatively identified as phloroglucinol derivative (eucaglobulin) [41]. Correspondingly, the second peak (t_R = 18.31 min.), [M-H] - 471.0833, released fragment ion in negative mode at *m/z* 453.6918 amu (M-CH_3) followed by m/z 427.23 amu (M-CH_3-CHOO), 219.4831 [globulol-3 H]. From the mass fragmentation of this compound, it could be of the formylated phloroglucinol derivative (Macrocarpal A). The third peak was spotted at (TR = 9.76 min.), with molecular ion peak $[M+H]^+$ 537. The fragmentation pattern of this compound showed sequential loss of hexose followed by OCH_2 corresponding to m/z 375 amu and 345.14 amu respectively. This fragmentation is in accordance with that of phloroglucinol glycoside derivative. This compound is likely identified as (cypellocarpin B) [15,41].

4.3. Hydroxybenzoic acid and Hydroxycinnamic acid derivatives

Concerning Hydroxybenzoic acid derivatives identified in the *E. camadulensis* ethanolic bark extract, a representative MS/MS spectrum of peak m/z 169 amu, (TR 9.6 min.) in the negative mode. The daughter ions detected at 124, 79 were due to the removal of (CHO_2), and M-CHO_2- CO_2) respectively, This confirmed the fragmentation pattern of GA [42]. The hydroxyl cinnamic acid derivatives were represented by two peaks at TR (10.66 & 12.23 min.) corresponding to the molecular ion peaks [M-H] 353.269 & [M-H] 195.5016 respectively. The former peak, yielded deprotonated Quinic acid (*m/z* at 191amu), in addition to another major ion corresponding to the Hydroxycinnamic acid residue at *m/z* 176.9 [caffeic acid-2 H]-. Consequently, this peak is tentatively identified as caffeoylquinic acid [43]. The latter peak exhibited a similar fragmentation pattern for ferulic acid with its characteristic peaks at m/z 178.7 amu [M-CH_3], followed by m/z 148.86 amu [M-CH_3-OCH_3]. Therefore, this compound is tentatively identified as ferulic acid [43]

4.4. Flavonoids

This class was represented by 6 compounds. Five of which were identified as flavonols and one as flavones.

4.4.1. Flavonols

Four flavonols were identified as Quercetin &Quercetin derivatives evident from fragments in their MS spectrum. The major identified detected compound peak TR = 12.86 min, with molecular ion peak m/z 610.5981 $[M+H]^+$. The MS^2 of this compound gave a strong peak at m/z 301.0876 amu which is equivalent to the loss of a hexose (-162) followed by a rhamanosyl moieties (-146) in addition to, 301 amu [M $+H^+$ - 146- 162 (hexosyl)] indicating the molecular ion of the aglycone quercetin. Accordingly, this compound is tentatively identified as Quercetin-rhamnosyl-hexosyl (Rutin) [44]. Likewise, another two peaks showing molecular ion peaks [M-H]- at *m/z* 433.01 and *m/z* 446.84 amu detected at t_R = 8.59 & 7.98 respectively. The characteristic ion peak for the Quercetin aglycone was distinguished in the mass spectrum of both compounds m/z 300.77 & 300.98 amu respectively. Hence, the first peak was recognized as Quercetin pentoside, [M-132]. The second peak was tentatively identified as quercetin-rhamnoside [M- 146]. Moreover, the peak observed at TR = 25.8 min evidenced its aglycone nature with [M-H] – 301. It showed fragment ions at 257.37, 229.17 & 185.08.This is in accordance with Quercetin aglycone. The fifth flavonol peak was detected at TR = 5.47 min. yielded m/z 460.60 [M-H]-. Its deprotonated fragments at *m/z* 399.0376 amu corresponding to the loss of rhamnosyl moiety from the molecular ion peak [M-146], followed by a peak with high intensity at m/z 315.33 amu, equivalent to (*iso*) rhamnetin aglycone could be identified as (*iso*) rhamnetin rhamnoside. Similarly, a peak was detected at TR = 26.63 min indicating its aglycone nature and was similar to (*iso*) rhamnetin aglycone with MS^2 fragments m/z 302.05 amu [M- CH3]. Therefore, this was also tentatively identified as (*iso*) rhamnetin [45].

4.4.2. Flavones

This was represented by one peak at the end of the chromatogram indicating its aglycone nature. These were identified as luteolin; [M-H] 287.0693 amu, with the characteristic daughter ions at m/z 268.91 amu corresponding to [M- OH].

Observing the HPLC profile of the 70% ethanolic extract of the barks against seven standards revealed the presence of Rutin as a major compound. Other compounds were detected as minors: Quercetin, *Epi* catechin, and Ellagic acid as compared to the retention time of the standards.

On the other hand, the analysis of the LC-MS/MS chromatogram for the ethanolic EBE showed phenolic compounds of different classes, the major of which were the flavonoids of the Quercetin derivatives. Rutin (12%), was the major identified compound. This is in agreement with the HPLC. Furthermore, phloroglucinol compounds – characteristic for genus Eucalyptus- were present in high amount, where eucaglobulin (11%) was the major identified phloroglucinol. Since, standardization of herbal extracts is a crucial step required so that uniform products can be prepared for clinical trials. Accordingly, the extract was standardized using Rutin. The percentage of Rutin in the extract was 1.26%. Moreover, the total phenolics & flavonoids in the extract were 434.8 mg/g GA equivalent ± 35.4 & 346.3 mg / g Rutin equivalent ± 0.03, respectively. All these results support the potential of the extract as a good antioxidant tool for ageing deterrence [46,47]. Choi et al. 2014 [48] studied the impact of Rutin *in vivo* on inflamed mouse skin induced by UVB. They reported that the topical use of Rutin on mice skin 30 minutes before being exposed to UVB irradiation resulted in improvement of epidermal hyperplasia and levels of proteins. In addition, expression of cyclooxygenase-2 (COX-2) and inducible nitric oxide synthase induced by ultra violet UVB was significantly inhibited. Another study conducted [49] evidenced that when Rutin (10% w/w) was incorporated in an oil-water emulsion, sun protection factor (SPF) values were raised to 30.

The phenolic compounds identified in EBE exert a significant role in the AgNPs biosynthesis. Thereby, they act as reducing agents and stabilizers due to the hydroxyl groups and their dendritic macrostructure. Additionally, the 3′-4′ hydroxyl system in the Quercetin and its

derivatives recognised in EBE imparts acidity which results in conversion into a keto group (48). Moreover, the green synthesis method used for nanoparticles preparation is eco-friendly, cheap and is more advantageous over other methods [30].

4.5. Silver nanoparticles

In the current study, Rutin was the major constituent in the extract as confirmed by HPLC fingerprint of the extract (Supplementary 2), so it is considered as a marker for the presence of the extract. Thereby, its presence indicated that the extract was loaded on AgNPs(loading capacity was 28 μg/mL) as shown in HPLC chromatogram which tested the major constituent unloaded from the AgNPs (Supplementary 4). This agrees with Singh et al who proposed that during AgNps formation phytoconstituents may interact with metal ions that my result in new compounds that exert the action [25]. The AgNPs had a size of 468.7 nm and this agrees with Prabha et al. [50].Several factors affect particle size as temperature, seed concentration, pH and reducing agent [25]. Further research can work on reaction conditions to optimize the resulting particle size for optimal effects.

4.6. Biochemical testing

Recent studies have highlighted the assosciation of apoptosis and senescence to ageing [3–5].In the current study, both EBE and AgNPs expressed significant difference in % of cells at G2/M phase, no significant difference between them and normal cells and were more potent than ascorbic acid. Moreover, both (treatment potential) expressed a decline in apoptotic cells % compared to aged ones with more potency than ascorbic acid itself.These findings agree with Cavinato et al study [51]. This highlights the potential of EBE and AgNps as anti-apoptotic and hence anti-ageing.

In our study, it was observed that both EBE and AgNPs used as treatment exhibited significant decrease in p53 and p21expression compared to aged cell. Moreover, they were more potent than the positive control itself. This is in accordance with a previous study done by Lim et al [52]. This goes in line with p53 is a transcription factor regulating various functions including growth arrest, DNA repair and apoptosis. When external or cellular stress occur inducing DNA damage, p53 degradation is inhibited. High level of p53 may accelerate the ageing process by inducing excessive apoptosis [53]. The p21 (known as cyclin-dependent kinase inhibitor1) has been shown to be up regulated during senescence [54]. Furthermore, studies have shown that p21 is the 1st mediator of downstream p53 dependent cell cycle arrest as a result of DNA destruction. Hence, deficiency of p21 retracts senescence [53].

The p16 ^{INK4a} is typically repressed in the absence of stress. Its increase in expression serves as a marker of senescence due to its effects on retinoblastoma protein and p53-mediated responsive pathways. Thereby, it serves as a good marker of ageing [55,56]. This is in accordance with our study where both EBE and AgNPs as treatment exhibited significant decrease in p16 ^{INK4a} levels compared to aged cells. Furthermore, they were more effective than positive control and posed no difference from normal cells.

Human telomerase is made up of a catalytic subunit and ribonucleic acid template. Telomerase provides de novo TTAGGG repeats to the ends of telomeres. As a result, telomere shortening and DNA breaks are prevented [57,58]. Both EBE and AgNPs whether treatment or prophylactic exhibited significant increase in telomerase compared to aged cells and were more potent than ascorbic acid. However, treatment potential was more potent than prophylactic potential with S3 and S4 in increasing telomerase concentration. This agrees with the reduction in telomerase will lead to DNA breaks which sequentially can prompt apoptosis or cellular senescence. This is mainly through p53-mediated expression of p21 [59]. Moreover, several *in vitro* studies have correlated telomere shortening to senescence [57,58].

Elastase, collagenase and tyrosinase enzymes are concerned with skin's elasticity, strength and whitening, respectively. Consequently, inhibiting the three enzymes can increase the skin strength, elasticity and prevent appearance of dark spots thus preventing the wrinkle formation [10]. Both EBE and AgNPs, exhibited comparable inhibitory effects against anti-wrinkle enzymes.This agrees with [26]. Elastase tends to breakdown collagen and elastin fibrils, at the valine side [60–62]. The polyphenol and flavonoid compounds carry hydroxyl groups that can bind to the carboxyl groups of the serine residue present at elastase active site. This results in the change of the enzyme mechanism of action. Consequently, this greatly helps in avoiding loss of skin elasticity and wrinkle formation [63]. Collagenase inhibition is attributed to either the interaction between the hydroxyl groups or the benzene ring present in phenolics with the collagenase functional groups. This leads to conformational changes and results in decreasing enzyme activity [62]. Additionally, metal chelators as phenolic acids, flavonoids and tannins can bind to the Zn in collagenase active site. Thereby, they inhibit its activity [64]. Moreover, tyrosinase catalyzes the first two regulatory steps of melanin biosynthesis [65]. Thus, any disturbance in tyrosinase expression and/or activity results in skin pigmentation diseases..Examples of which are; lentigo senilis, urticaria pigmentosa, and age-related skin hyperpigmentation [35]. Consequently, tyrosinase inhibitors are endowed with skin-whitening activity. Besides, hydroxyl groups of inhibitors bind to tyrosinase active site causing conformational changes leading to enzyme inhibition [66]. It is worth mentioning that the previous approaches for three enzyme inhibition mechanisms are further confirmed by the significant and positive correlation between the total phenolic and flavonoid contents and the anti-ageing enzymes.

5. Conclusion

Both EBE and its corresponding AgNps are anti-ageing candidates as they inhibit apoptosis, senescence and prevent skin whitening and wrinkle formation. EBE exerted anti-wrinkle activity due to its high phenolic content. At the same time loading of the extract on AgNPs maintains the activity. In this sense, we hereby provide a cost effective, eco-friendly, affordable technique for synthesis of AgNPs using EBE instead of being shed as waste. These findings highlight the importance of reusing waste for the progress of commercial skin care formulations. However, further *in vivo* and clinical trials are recommended and comparison to other anti- wrinkle treatments formulations are prerequisites.

6. Statement of Authorship

I am an author on this submission, have adhered to all editorial policies for submission as described in the Information for Authors, attest to having significantly participated in the study that is reported as well as made substantial contributions to the first concept and design or analysis and interpretation of data and second, writing the manuscript or revising it critically for content, and declare no conflict of interest and no financial disclosures.

Funding

This research did not receive any specific grant from funding agencies in the public, commercial, or not-for-profit sectors.

Conflict of Competing Interest

The authors declare that they have no known competing financial interests or personal relationships that could have appeared to influence the work reported in this paper.

Acknowledgement

No acknowledgements to be made

References

[1] D. McHugh, J. Gil, J. Cell Biol. 217 (2017) 65–77.
[2] T. Niccoli, L. Partridge, Curr. Biol. 22 (2012) R741–R752.
[3] D. Muñoz-Espín, A.M. Cañamero, G. Maraver, J. Gómez-López, S. Contreras, A. Murillo-Cuesta, I. Rodríguez-Baeza, J. Varela-Nieto, M.C. Ruberte, M. Serrano, Cell 155 (2013) 1104–1118.
[4] D. Muñoz-Espín, M. Serrano, Nat. Rev. Mol. Cell Biol. 15 (2014) 482–496.
[5] J. Tower, Ageing Res Rev. 23 (2015) 90–100.
[6] V.L. Ernster, D. Grady, R. Miike, D. Black, J. Selby, K.J.A.j.o.p.h. Kerlikowske, 85 (1995) 78-82.
[7] A.J.W.J.P. Shehada, 3 (2014) 528-544.
[8] Y.-S. Ho, K.-F. So, R.C.-C.J.A.r.r. Chang, 9 (2010) 354-362.
[9] C. Mathen, R. Thergaonkar, M. Teredesai, G. Soman, S.J.I.J.H.M. Peter, 2 (2014) 95-99.
[10] T. Shoko, V.J. Maharaj, D. Naidoo, M. Tselanyane, R. Nthambeleni, E. Khorombi, Z. J.B.c. Apostolides, a. medicine, 18 (2018) 54.
[11] S.n.A. Santos, C.S. Freire, M.R.M. Domingues, A.J. Silvestre, C.P.J.J.o.a. Neto, f. chemistry, 59 (2011) 9386-9393.
[12] E. Conde, E. Cadahia, R. Diez-Barra, M.J.H.a.R.-u.W. García-Vallejo, 54 (1996) 175-181.
[13] B.R. Ghalem, B.J.A.j.o.P. Mohamed, pharmacology 2 (2008) 211–215.
[14] M.A. Ghareeb, M.R. Habib, H.S. Mossalem, M.S.J.B.o.t.N.R.C. Abdel-Aziz, 42 (2018) 16.
[15] A.-N. Singab, N. Ayoub, E. Al-Sayed, O. Martiskainen, J. Sinkkonen, K.J.R.o.N.P. Pihlaja, 5 (2011).
[16] F.M. Soliman, M.M. Fathy, M.M. Salama, A.M. Al-Abd, F.R. Saber, A.M.J.S.r. El-Halawany, 4 (2014) 5410.
[17] D.J.N.J.o.B. Musa, M. Biology 31 (2016) 53–64.
[18] R. Seqqat, L. Blaney, D. Quesada, B. Kumar, L. Cumbal, J. Nanotechnol. (2019) 1–2.
[19] S. Iravani, H.S. Korbekandi, V. Mirmohammadi, B. Zolfaghari, Res. Pharm. Sci. 9 (2014) 385–406.
[20] L.C.S. Lopes, L.M. Brito, T.T. Bezerra, K.N. Gomes, F.A.D.A. Carvalho, M.H. Chaves, W. Cantanhêde, An. Acad. Bras. Cienc. 90 (2018) 2679–2689.
[21] H.F. Aritonang, H. Koleangan, A.D. Wuntu, International Journal of Microbiology 2019 (2019) 1–8.
[22] A. Roy, O. Bulut, S. Some, A.K. Mandal, M.D. Yilmaz, RSC Adv. 9 (2019) 2673–2702.
[23] J. Kesharwani, K.Y. Yoon, J. Hwang, M.J. Rai, Bionanoscience 3 (2009) 1–6.
[24] S. Onitsuka, T. Hamada, H. Okamura, Colloids Surfaces B Biointerfaces 173 (2019) 242–248.
[25] H. Singh, J. Du, P. Singh, T.H. Yi, Journal of Nanostructure in Chemistry 8 (2018) 359–368.
[26] E. Mostafa, M.A.A. Fayed, R.A. Radwan, R.O. Bakr, Colloids and Surfaces B: Biointerfaces 182 (2019).
[27] S. Kaul, N. Gulati, D. Verma, S. Mukherjee, U. Nagaich, Journal of Pharmaceutics 2018 (2018).
[28] E.J.O.L.S. Attard, 8 (2013) 48-53.
[29] T.J. Herald, P. Gadgil, M.J.J.o.t.S.o.F. Tilley, Agriculture 92 (2012) 2326–2331.
[30] R. Kumar, l.G. Ghosha, A. Jain, M. Goyal, Journal of J Nanomedicine & Nanotechnology 8 (2017) 4.
[31] S.Y. Wen, J. Chen, W. Y.S, R. Aneja, C.J. Chen, C.Y. Huang, W.W. Kuo, Environ Toxicol. 32 (2017) 2419–2427.
[32] J. Bieth, B. Spiess, C.G. Wermuth, Biochemical Medicine 11 (1974) 350–357.
[33] J.A.E. Kraunsoe, T.D.W. Claridge, L.G, Biochemistry 35 (1996) 9090–9096.
[34] R. Rauniyar, M. Talkad, S. Sahoo, A. Singh, P. Harlalka, International Journal of Innovative Research in Science, Engineering and Technology 3 (2014) 14259–14266.
[35] A. Slominski, D.J. Tobin, S. Shibahara, J. Wortsman, Physiol. Rev. 84 (2004) 1155–1228.
[36] C. Wyrepkowski, D. Gomes da Costa, A. Sinhorin, W. Vilegas, R. De Grandis, F. Resende, E. Varanda, L.J.M. dos Santos, 19 (2014) 16039-16057.
[37] M.J. Simirgiotis, G.J.J.o.F.C. Schmeda-Hirschmann, Analysis 23 (2010) 545–553.
[38] L.d.L. Teixeira, F.C. Bertoldi, F.M. Lajolo, N.M.A.J.J.o.a. Hassimotto, f. chemistry 63 (2015) 5417–5427.
[39] M. Zhu, X. Dong, M.J.M. Guo, 20 (2015) 22463-22475.
[40] T. Yoshida, Y. Amakura, M.J.I.j.o.m.s. Yoshimura, 11 (2010) 79-106.
[41] L. Boulekbache-Makhlouf, E. Meudec, M. Chibane, J.-P. Mazauric, S. Slimani, M. Henry, V. Cheynier, K.J.J.o.a. Madani, f. chemistry 58 (2010) 12615–12624.
[42] P. Mena, L. Calani, C. Dall'Asta, G. Galaverna, C. García-Viguera, R. Bruni, A. Crozier, D.J.M. Del Rio, 17 (2012) 14821-14840.
[43] J. Sun, F. Liang, Y. Bin, P. Li, C.J.M. Duan, 12 (2007) 679-693.
[44] R.M. Ibrahim, A.M. El-Halawany, D.O. Saleh, E.M.B. El Naggar, A.E.-R.O. El-Shabrawy, S.S.J.R.B.d.F. El-Hawary, 25 (2015) 134-141.
[45] Ł. Marczak, P. Znajdek-Awiżeń, W.J.M. Bylka, 21 (2016) 1229.
[46] C.H. Kang, S.J. Rhie, Y.C.J.T.r. Kim, 34 (2018) 31.
[47] B. Quéguineur, L. Goya, S. Ramos, M.A. Martín, R. Mateos, L.J.F. Bravo, c. toxicology 50 (2012) 2886–2893.
[48] K.-S. Choi, J.K. Kundu, K.-S. Chun, H.-K. Na, Y.-J.J.A.o.b. Surh, biophysics 559 (2014) 38–45.
[49] B. Choquenet, C. Couteau, E. Paparis, L.J.J.J.o.n.p. Coiffard, 71 (2008) 1117-1118.
[50] S. Prabha, G. Arya, R. Chandra, B. Ahmed, S. Nimesh, Artificial Cells, Nanomedicine, and Biotechnology 44 (2014) 83–91.
[51] M. Cavinato, B. Waltenberger, G. Baraldo, C.V.C. Grade, H. Stuppner, P.J. Durr, Biogerontology 18 (2017) 499–516.
[52] E.G. LIM, E.T. Kim, B.M. KIM, E.J. Kim, S.-Y. KIM, Y.M. KIM, Molecular medicine reports 17 (2018) 2572–2580.
[53] A. Rufini, P. Tucci, I. Celardo, G. Melino, Oncogene 32 (2013) 5129–5143.
[54] X.D. Wang, E. Lapi, A. Sullivan, I. Ratnayaka, R. Goldin, R. Hay, et al., Cell Death Differ 18 (2011) 304–314.
[55] J. Krishnamurthy, et al., J. Clin. Invest 114 (2004) 1299–1307.
[56] A. Satyanarayana, K.L. Rudolph, J. Clin. Invest. 114 (2004) 1237–1240.
[57] D.M. Baird, J. Rowson, D. Wynford-Thomas, D. Kipling, Nat Genet. 33 (2003) 203–207.
[58] F.A. Di Fagagna, P.M. Reaper, L. Clay-Farrace, H. Fiegler, P. Carr, T. VonZglinicki, G. Saretzki, P. Nigel, C.S.P. Jackson, Nature 426 (2003) 194–198.
[59] G. Morgan, Research and Reports in Biochemistry (2013) 71–78.
[60] H. Bigg, I. Clark, C. TE, Biochim Biophys Acta 1208 (1994) 157–165.
[61] L.C. Cefali, J.A. Ataide, P. Moriel, M.A. Foglio, P.G. Mazzola, Int. J. Cosmet. Sci. 38 (2016) 346–353.
[62] B. Madhan, G. Krishnamoorthy, J.R. Rao, N. BU, Int J Biol Macromol. 41 (2007) 16–22.
[63] G. Iván, Z. Szabadka, R. Ordög, V. Grolmusz, N.-S. G, Biochem Biophys ResCommun 383 (2009) 417–420.
[64] M. Mc Donald, I. Mila, A. Scalbert, J Agric Food Chem. 44 (1996) 599–606.
[65] T. Pillaiyar, M. Manickam, V. Namasivayam, J. Enzyme, Inhib. Med. Chem. 32 (2017) 403–425.
[66] S.B. Heung, S.R. Ho, W.Y. Jae, M.A. Soo, Y.L. Jin, M.K. Jeonga-Lee, H.K. Kim, S.C. Ih Duck, Bull. Korean Chem. Soc 29 (2008) 43–46.